DMU

Journal of Interdisciplinary Studies 7(2023) 1025-1036

Journal homepage: www.jims.dmu.edu.et

Volume 7(2), Dec 2023

DMU-JIDS

Nanomaterial Based Digital Probe Design and Development for Basal Body Temperature Measurement

Almaw Ayele Aniley[1,*]

[1]Department of Electrical and Computer Engineering, Institute of Technology, Debre Markos University, Debre Markos, Ethiopia

[*]Corresponding Author's Email: lingerayele@gmail.com, almaw_ayele@dmu.edu.et

Abstract

In this paper, a Basal Body Temperature monitoring Internet of Things-enabled system is fabricated by using a thermistor constructed from nanomaterial. Basal Body Temperature is the lower most temperature of the human body who is at break and varies from 96°F-99.5°F. A nanoceramic powder-based thermistor is fabricated by pressing the self-synthesized $NiMn_2O_4$ *nanomaterial powder in an insulated cylindrical tube with aluminium electrodes. The mean crystallite size of the nanoceramic powder is found to be 27 nm. This result is obtained from the x-ray diffraction characterization results with the help of Scherr's model. Sensor calibration is performed by using a thin film heater, a combination of LM35 and a fabricated thermistor with Atmega328 microcontroller. Further Internet of Things-enabled Basal Body Temperature monitoring system is fabricated with the use of an open Internet of Things platform. The fabricated system effectively measures Basal Body Temperature with a precision of about four digits, which is better suitable for forecasting the ovulation period in humans by the analysis of the two-phase temperature trend of the Basal Body Temperature graph. This information has been helpful in order to naturally become pregnant or not. Fertility awareness method facilitates natural family planning.*

Keywords: *Thermistor, Nanoceramic, IoT, Basal Body Temperature, Ovulation detection*

1. Introduction

The degree of heat intensity is measured by temperature. The temperature of a body is an expression of its molecular excitation(Ling et al., 2015). It is among the most frequently seen environmental parameters given that the majority of mechanical, chemical, biological, electrical, and physical systems show some sort of temperature dependence(Sumriddetchkajorn & Chaitavon, 2009).

The widely accepted typical adult temperature in a healthy state is about 98.6°F (Hutchison et al., 2008). The normal temperature of a human is generally 97.7°F to 99.5°F (Hutchison et al., 2008). The temperature of the human body is a complex, non-linear variable that is both internally and externally influenced by a variety of factors, including age, effort, infection, gender, the location of the measurement in the body, the time of day it is taken, the subject's level of consciousness, activity, emotional state, psychological factors, inadequate and irregular sleep schedule, and the subject's reproductive status.(Mackowiak et al., 1992)'(Grodzinsky, 2013)'(Lu & Dai, 2009).

Human body temperature is measured using various kinds of thermometers, including analogue clinical thermometers (mercury thermometers), digital thermometers, tympanic membrane thermometers and thermometer probes. The following places are used to measure the temperature of a human body: the mouth, the rectum, the vagina, the bladder, the nose, the forehead, above the temporal artery, under the arm, the ear, and the tympanic temperature(Märtha Sund-Levander RN, MSc et al., 2002)'(Kelly G, 2006). There are different ways to determine body temperature in a variety of parts of the body and give different results.

Humans are homoeothermic, the bioprocesses, functions and body temperature have been verified at every level of organization to possess regular, time-sensitive fluctuations known as biological rhythms(Smolensky & Alonzo, 1993)'(Kelly, 2006). Body temperature varies within the day with the largest in the late afternoon (4:00 and 6:00 p.m.) and the smallest levels about 4 a.m. following the Circadian rhythms(Kelly G, 2006)'(Baker et al., 2001). This smallest temperature is attained typically once the body becomes at rest which is known as Basal Body Temperature (BBT).

The temperature of the human body is sensitive to many hormones indicating the events taking place in the human body. The temperature rhythm variations during the menstrual cycle in women are called circa mensal rhythm(Kelly, 2006). At follicular stage of the menstrual cycle, Basal Body Temperature reaches its smallest point about 1 day earlier ovulation because of a larger amount of estrogen, later ovulation, a larger amount of progesterone generated by the corpus luteum basal body temperature increases abruptly later ovulation to about 0.5 -1℃ during the luteal phase, the event is referred to as Biphasic Temperature Pattern(Su et al., 2017).

The currently available methods for measuring basal body temperature are mercury thermometers with the disadvantages of less accuracy and precision, easy breakage, slow response and hazardous due to the presence of toxic mercury (Hg); digital thermometers are also used as basal thermometer which has less precision and accuracy and the results are unreliable(Dolkar et al., 2013) and other basal thermometers available which are accurate, precise and capable of storing data but, it is very expensive.

Charting of biphasic temperature form of Basal Body Temperature is applicable as a part of the Fertility Awareness Method of Natural Family Planning(NFP) known as the Symptothermal method which is the simplest, harmless and non-invasive efficient mechanism to sense ovulation by following the symptoms and signals of a human body(Fehring, 2004)'(Smoley et al., 2012). The exact prediction of ovulation, as a pointer aids to accomplish or protect pregnancy naturally (Pallone & Bergus, 2009)'(Watanabe et al., 2016).

In this work, a nanoceramic powder-based thermometer is fabricated, characterized, calibrated and tested. The $NiMn_2O_4$ nanomaterial is prepared using a solution technique. The thermistor from this nanoceramic powder is fabricated using a simple and economical method and the resulting thermistor is stable, highly accurate and more precise. The basal body temperature displaying system is manufactured using the fabricated thermistor, Atmega328 microcontroller, and Arduino Integrated Development Environment (IDE). Further, this system is upgraded with IoT using NodeMCU, ThingSpeak IoT platform and Arduino IDE, to simplify the broadcast, storage, access, processing and plotting of the information in real time and also help the involvement of health professionals for the correct real time measurement of ovulation period as the Biphasic temperature pattern variations are only around 0.5℃ - 1℃ and the distinction of temperature variations due to the influence of others factors demands specialization. So the developed IoT system is very convenient for BBT monitoring with high accuracy and precision of more than 3 digits privileging the prediction of the ovulation period.

2. Experimental

2.1.Chemicals Used

To synthesize $NiMn_2O_4$ nanomaterial tetra-hydrated Nickel acetate($C_4H_{14}NiO_8.4H_2O$), tetra-hydrated Manganese acetate($(CH_3COO)_2Mn\cdot 4H_2O$), Oxalic acid($C_2H_2O_4$) and Distilled water(H_2O) have been utilized. These chemicals have been bought from Sigma Aldrich.

2.2.Equipment used

To prepare and characterize the resulting nanomaterial Alumina crucible, mortar and pestle, beakers, magnetic stirrer beads, digital and programmed hot plate, muffle furnace, fumehood, powder XRD and FeSEM/EDS have been utilized. All these equipment are found in Mangalore University, Mangalore, India. I have experimented in the Department of Electronics, Mangalore University, Mangalore, India research lab.

$NiMn_2O_4$ nanomaterial is prepared using a modified solution route technique. Two hundred milligrams (mgs) of $C_4H_{14}NiO_8.4H_2O$ and 393.9 mgs of $(CH_3COO)_2Mn\cdot 4H_2O$ have been mixed and dissolved in 0.24 liters(l) of solvent which is distilled water. The sample is put in a magnetic stirrer on a hot plate at a heating temperature of about 45℃ and a time duration of half an hour. 70 mgs of $C_2H_2O_4$ is dissolved in 0.10 l of solvent in a glass beaker kept in a fumehood at room temperature. The resulting solution is mixed with the former solution with vigorous stirring. Then the resultant sample is kept at 75℃ until a thick sol is obtained. The whole experiment took place in a fumehood. Then the resulting sol is dried in the furnace at 105℃. The dried sample powder has been ground with a pestle and mortar. Finally, it has been calcined in a furnace at 960℃ for about 190 minutes.

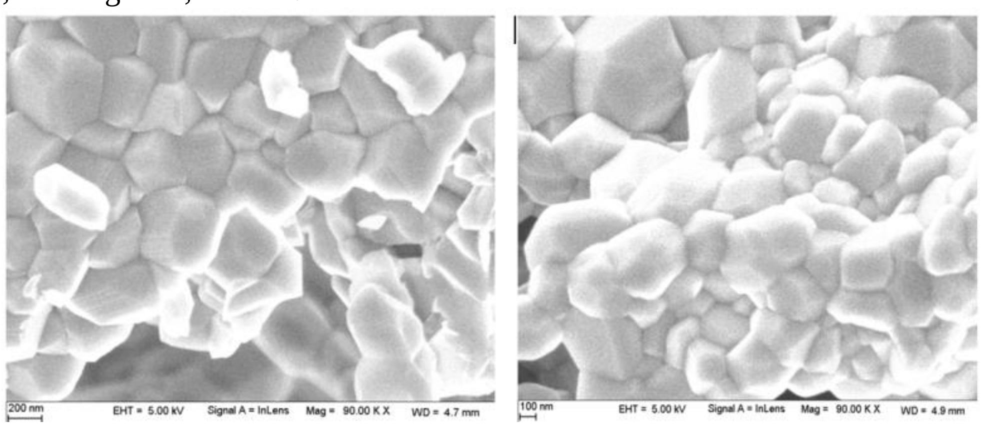

Figure 1. FeSEM Micrograph of the nanomaterial $NiMn_2O_4$ sample

Field emission scanning electron microscopy with energy dispersive spectroscopy(FeSEM/EDS) and powder x-ray diffractometer (XRD) have been utilized to describe the surface morphology and mean crystallite size, constituents, and crystal arrangement of the resultant nanopowder correspondingly.

3. Results and Discussion

3.1.Results and discussion for the nanoceramic $NiMn_2O_4$ powder

FeSEM

It is used for characterizing the morphology and particle size of the synthesized powder.

The FeSEM image of the resulting ceramic powder is shown in Figure 1. As shown in this figure, the nanomaterial is fabricated by wet chemical method using distilled water as a solvent, synthesized $NiMn_2O_4$ nanoceramic powder consists of distinct nanoceramic grains with some agglomeration and the resulting samples are homogeneous. The resultant grains are composed of nanocrystallites. The agglomeration is created due to the moisture, characteristics of the material and the calcination temperature. The mean grain size of the sample is 54nm and the mean particle size is about 35nm.

EDS

The chemical composition analysis of the resulting sample is performed using EDS with the K-lines of the respective elements on a well-crystallized powder. The cation ratio of Ni: Mn is found to be 1:1.96 which is in good agreement with the expected 1:2 proportion. EDS result also confirms that the powder sample contains Ni, Mn and O_2 as shown in Figure 2.

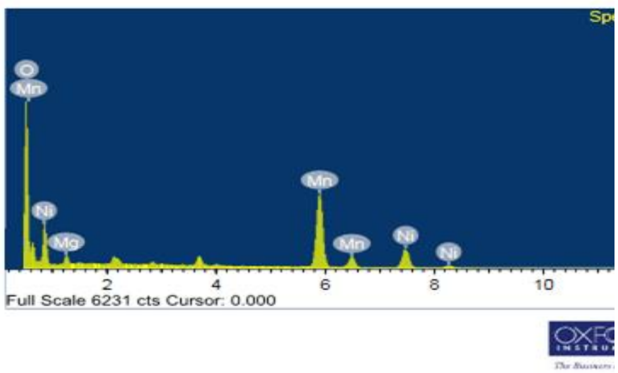

Figure 2. EDS analysis of the sample

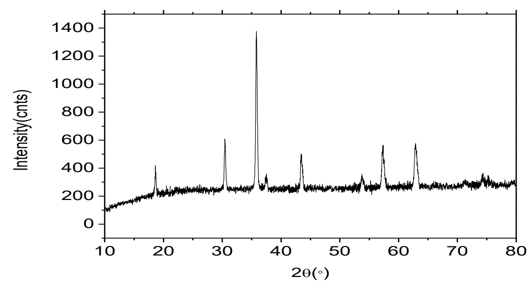

Figure 3. XRD pattern of the resulting powder

XRD

The elements of K_α Drawings have been logged in the step-scanning mode, with a (2θ) step of 0.02º scan and 2 seconds per step counting time in the range of $10^0 \leq 2\theta \leq 80^0$. As shown in Figure *3*, there have been nine peaks shown during the experiment. Among the peaks the longest (2957.91 cps) has been seen at 35.96º with 0.2492º Full-width half maximum(FWHM) while the shortest peak (196.89cps) has been seen at 76.06116º with 0.2106º FWHM.

Powder XRD has been used to measure the mean crystallite size of nanopowder from the resulting diffracted pattern using XRD results and the Scherrer equation from equation (1).

$$D = \frac{0.9 * \lambda}{\beta * cos(\theta)} \qquad (1)$$

Where β is the FWHM of the diffraction peak in radians, θ is the Bragg's angle, and λ is the CuKα source's x-ray wavelength (0.154059nm). The nanoceramic material's mean crystallite size has been measured at 27 nm.

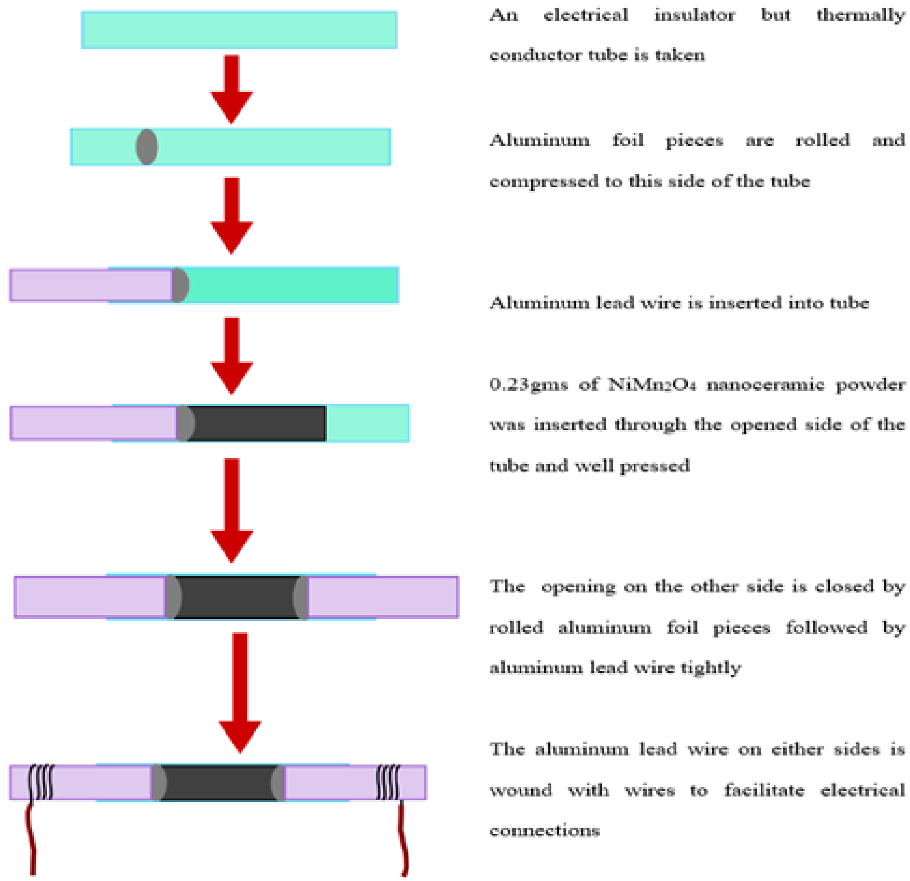

Figure 4. Sensor fabrication process

3.2.Thermistor fabrication and calibration result

The detailed fabrication process steps of the sensor are clearly shown in Figure 4. The thermistor is fabricated using the prepared $NiMn_2O_4$ nanomaterial using a cylindrical tube of thermally conducting and electrically insulating material. The resulting discrete thermistor is shown in Figure 5.

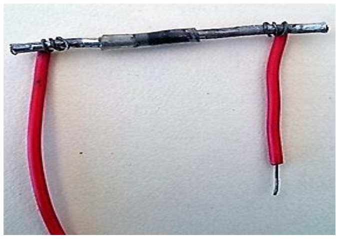

Figure 5. Fabricated thermistor

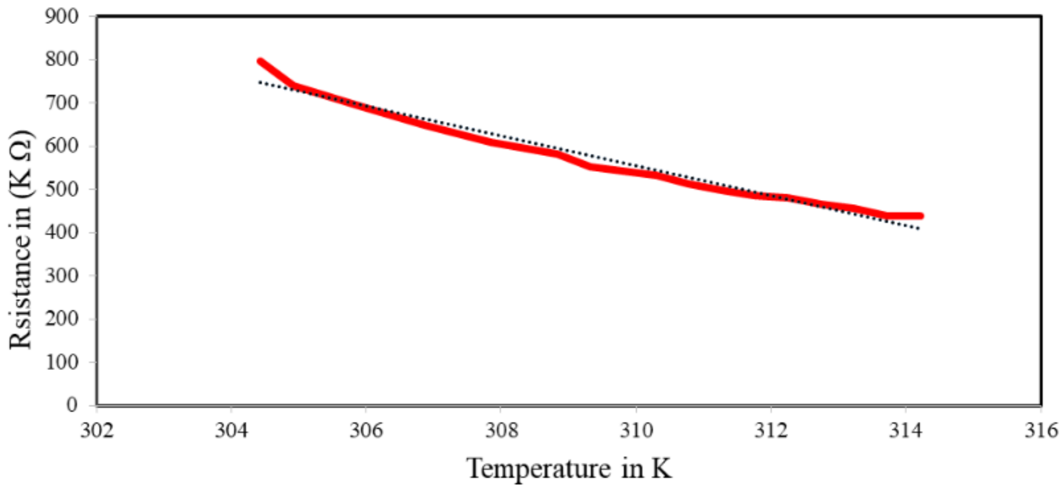

Figure 6. Temperature versus resistance of the thermistor

Adjusting the value of the fabricated sensor

The resulting thermistor is characterized and calibrated using a homemade circuit interfacing the fabricated sensor with an Atmega328 microcontroller, LM35 IC temperature sensor, FTO-coated glass electric heater and digital multimeter. Temperature versus resistance graph of the thermistor is shown in Figure 6. The thermistor was calibrated using the β-coefficient model of thermistors with the characteristic results. The value of R_0 is 1.02 MΩ and the β-coefficient value is 5520K. The thermistor model is found to be as shown in equation(2).

$$\frac{1}{(T(k))} = \frac{1}{305.15} + \frac{1}{\beta} * ln\left(\frac{R}{1.02\mathrm{M}\Omega}\right) \qquad (2)$$

Embedded system development and testing

Development of BBT monitoring system

An Atmega328 microcontroller, a 2X16 LCD, the Arduino IDE, a basic voltage divider circuit for signal conditioning, and a ready-made temperature sensor are used in the development of the embedded system for BBT monitoring. A straightforward voltage divider electric circuit is used to condition the thermistor-sensed signal so that the microcontroller may use it. The ADC output of the microcontroller in voltage is converted to resistance value. The obtained resistance values are transformed to temperature value of Fahrenheit scale using the β-coefficient model of thermistors equation as given in equation (2). The thermistor is improved in such a way that temperature can be easily measured. The diagram of the embedded structure is given in Figure *7*.

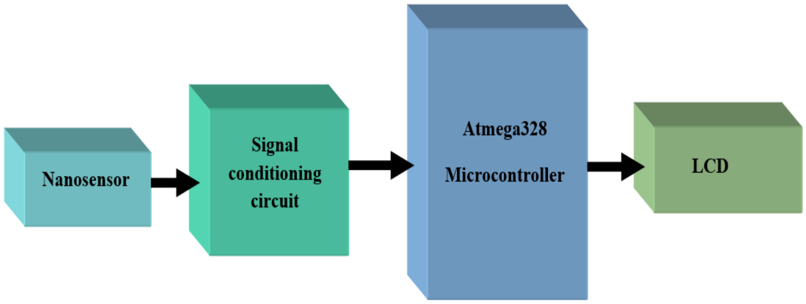

Figure 7. Developed embedded system in block diagram

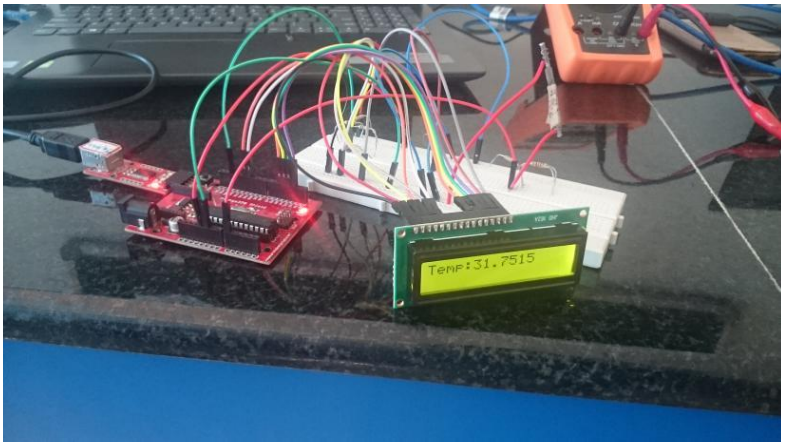

Figure 8. Prototype of the developed thermometer

The devised device can measure in the 20–50°C range with a precision of roughly four digits. The system's digital reading on the prototype is displayed in Figure 8.

Development of an IoT system for BBT monitoring

The BBT monitoring system has been designed using NodeMCU (ESP8266), ThingSpeak, an open-source platform, and IoT technology. Wi-Fi modules have been used instead of an external Wi-Fi module along with Atmega 328 microcontroller and programmed in Arduino IDE. ThingSpeak aids the creation of channels, collection and storing of the sensor data in the cloud and also provides applications that assist in the analysis and visualization of the obtained data.

The block diagram of the NodeMCU, thermistor and signal conditioning circuit is displayed in Figure 9. The thermistor that was made with a signal conditioning circuit is interfaced with NodeMCU and connected to the ThingSpeak server via a Wi-Fi connection, the sensed values are transmitted and stored in the ThingSpeak cloud in real time. The sensor values stored are accessible to the users in real time via smartphones and computers.

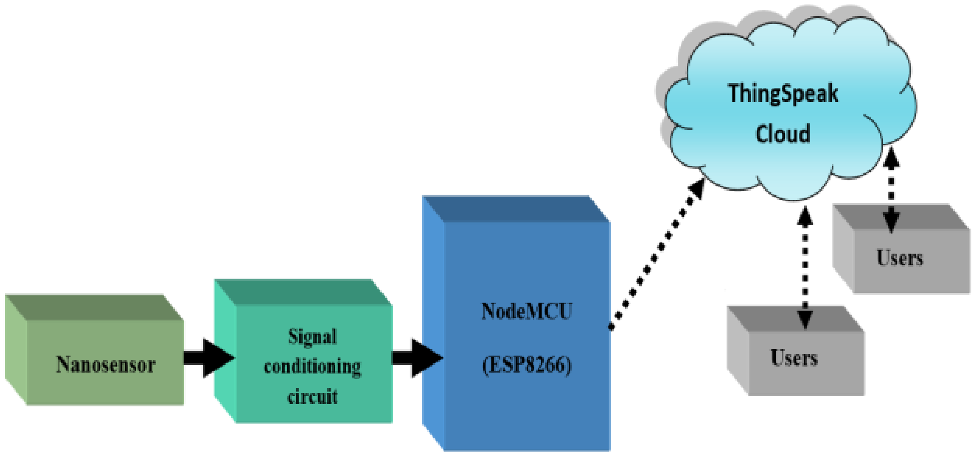

Figure 9. Block diagram of NodeMCU interfaced BBT monitoring system

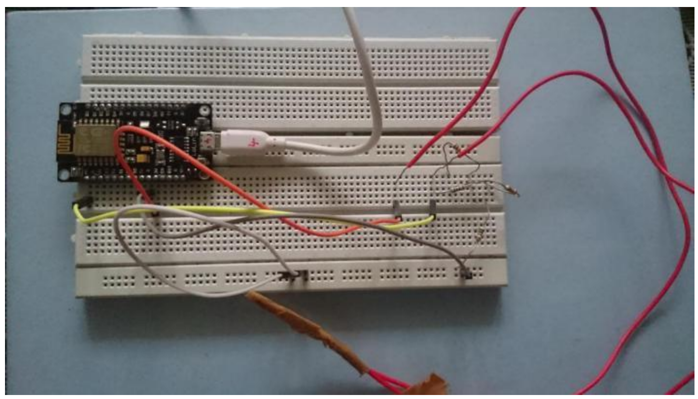

Figure 10. Prototype of NodeMCU interfacing with the fabricated thermistor

The resultant prototype of the developed IoT system for BBT monitoring using a signal-containing circuit, NodeMCU and the fabricated sensor is shown in Figure *10*.

BBT measurement

Readings from the developed thermometer have been taken during testing at the same time every day in the morning, between 4 and 5 am. A channel is constructed to submit the measured values to ThingSpeak. Read and write keys for an API are produced automatically once it has been created. Programming has made use of an API read key to update sensor data in real time in the channel with a certain API key. Through the use of a Wi-Fi connection that matches the program's specified SSID and password, the measured data is uploaded to ThingSpeak. The flow chart in Figure 11 explains how to use the Arduino IDE to post sensor values to the ThingSpeak cloud.

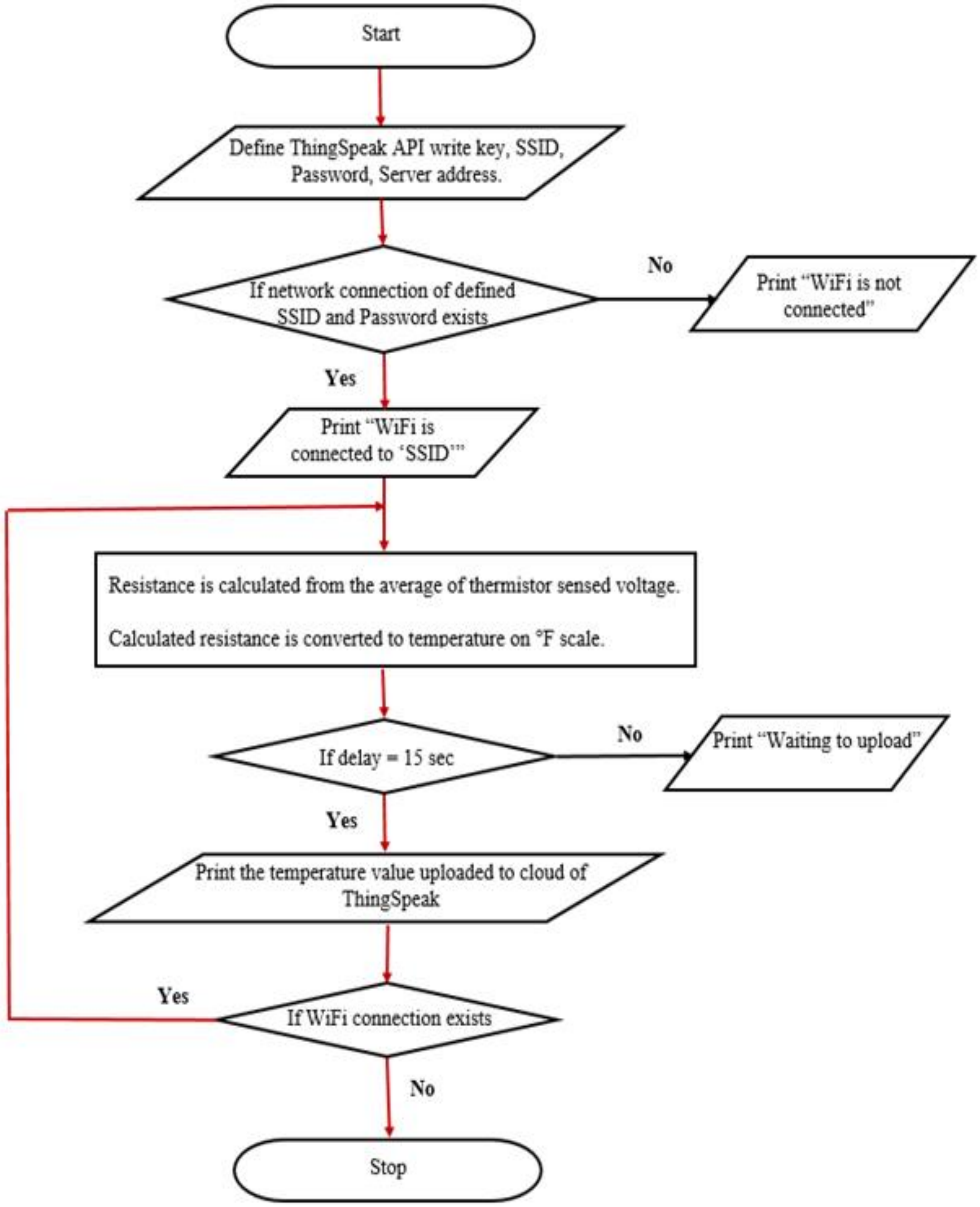

Figure 11. Sensor data uploading to ThingSpeak flowchart

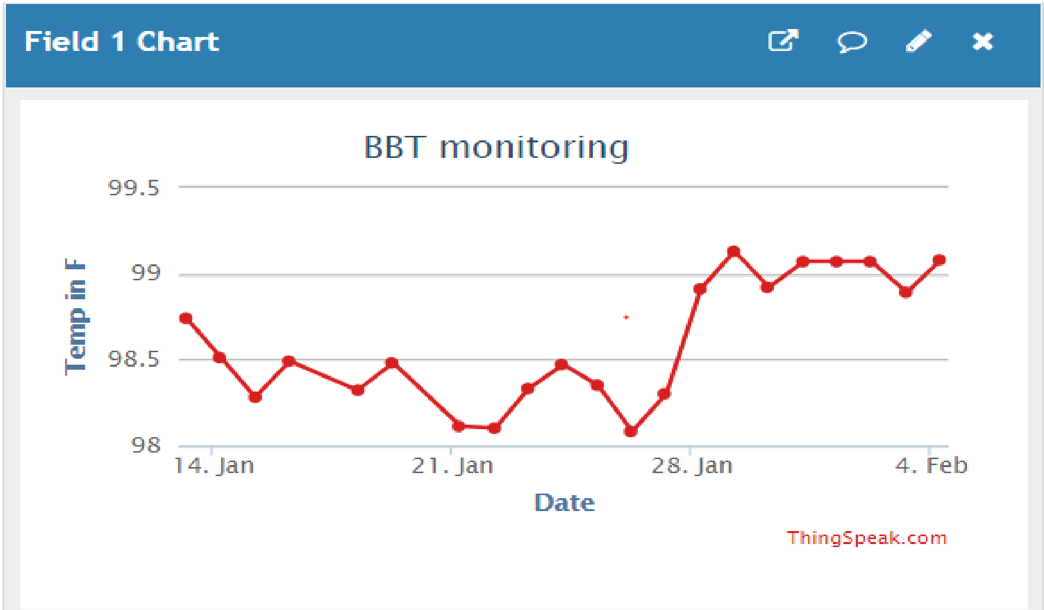

Figure 12. Biphasic pattern of women's BBT readings uploaded to ThingSpeak

Additionally, the thingSpeak platform allows uploaded data to be drawn with the date displayed in Figure 12. Examining this graph in the picture, we can see that the BBT is modest before ovulation and significant following ovulation, The BBT sharply rises to 98.91°F after falling by 98.08°F during the cycle's 15–17 days. Therefore, ovulation can be predicted to occur between January 26 and 28. ThingSpeak allows the exporting of the stored sensor data in the cloud in .json, .xml, or .csv formats, which can be further helpful in the detailed processing and analysis of sensor data in MATLAB or Excel spreadsheets to draw accurate conclusions.

4. Conclusion

Herein we report the $NiMn_2O_4$ nanoceramic powder-based thermometer was developed for the BBT monitoring system to estimate the ovulation period in human beings. The nanoceramic material which is $NiMn_2O_4$ has been prepared using a modified solution route technique. The thermistor has been fabricated by pressing the powder into an insulated cylindrical tube with aluminium electrodes. The variation of BBT throughout the menstrual cycle is not more than 0.5 - 1°C, therefore more precision and knowledge are needed for the estimation of ovulation. The resulting thermometer output shows about four-digit precision with a temperature range of 20-50°C. Furthermore, the fabricated embedded system enables the IoT to honour the involvement of health professionals for the correct detection of the ovulation period in real time. Thus, the symptothermal method of predicting ovulation in women is more accurate and enhances the efficiency and effectiveness of NFP. It is also possible to fabricate the resulting thermistor on a flexible substrate as a thin film to design and develop a wearable electronic system. Wearable electronic systems are flexible, easy and comfortable to install and use in real time with IoT devices.

References

Baker, F. C., Waner, J. I., Vieira, E. F., Taylor, S. R., Driver, H. S., & Mitchell, D. (2001). Sleep and 24 hour body temperatures: A comparison in young men, naturally cycling women and women taking hormonal contraceptives. *Journal of Physiology*, *530*(3), 565–574. https://doi.org/10.1111/j.1469-7793.2001.0565k.x

Dolkar, R., Kapoor, S., Singh, N. V., & Suri, V. (2013). A Comparative Study On The Recording Of Temperature By The Clinical Mercury Thermometer And Digital Thermometer. *Nursing and Midwifery Research Journal*, 1–12. https://doi.org/10.33698/nrf0148

Fehring, R. J. (2004). The future of professional education in natural family planning. *JOGNN - Journal of Obstetric, Gynecologic, and Neonatal Nursing*, *33*(1), 34–43. https://doi.org/10.1177/0884217503258549

Grodzinsky, E. (2013). *Assessment of body temperature measurement options*. *September*. https://doi.org/10.12968/bjon.2013.22.16.942

Hutchison, J. S., Ward, R. E., Lacroix, J., Hébert, P. C., Barnes, M. A., Bohn, D. J., Dirks, P. B., Doucette, S., Fergusson, D., Gottesman, R., Joffe, A. R., Kirpalani, H. M., Meyer, P. G., Morris, K. P., Moher, D., Singh, R. N., & Skippen, P. W. (2008). Hypothermia Therapy after Traumatic Brain Injury in Children. *New England Journal of Medicine*, *358*(23), 2447–2456. https://doi.org/10.1056/NEJMoa0706930

Kelly, G. (2006). Body temperature variability (part 1): A review of the history of body temperature and its variability due to site selection, biological rhythms, fitness, and aging. *Alternative Medicine Review*, *11*(4), 278–293.

Kelly G. (2006). "Body temperature variability (Part 1): a review of the history of body temperature and its variability due to site selection, biological rhythms, fitness, and aging". *Altern Med Rev*, *11*(4), 278–93.

Ling, T. H. Y., Wong, L. J., Tan, J. E. H., & Kiu, K. Y. (2015). Non-intrusive Human Body Temperature Acquisition and Monitoring System. *Proceedings - International Conference on Intelligent Systems, Modelling and Simulation, ISMS*, *2015-Octob*, 16–20. https://doi.org/10.1109/ISMS.2015.17

Lu, S. H., & Dai, Y. T. (2009). Normal body temperature and the effects of age, sex, ambient temperature and body mass index on normal oral temperature: A prospective, comparative study. *International Journal of Nursing Studies*, *46*(5), 661–668. https://doi.org/10.1016/j.ijnurstu.2008.11.006

Mackowiak, P. A., Wasserman, S. S., & Levine, M. M. (1992). A critical appraisal of 98.6 degrees F, the upper limit of the normal body temperature, and other legacies of Carl Reinhold August Wunderlich. *JAMA: The Journal of the American Medical Association*, *268*(12), 1578–1580. https://doi.org/10.1001/jama.268.12.1578

Märtha Sund-Levander RN, MSc, P. (Student), Christina Forsberg RN, P. (Senior L., & Lis Karin Wahren MLT, P. (Associate P. (2002). Normal oral, rectal, tympanic and axillary body temperature in adult men and women: a systematic literature review. *Scandinavian Journal of Caring Sciences*, *16(2)*, 122–128. https://doi.org/https://onlinelibrary.wiley.com/doi/abs/10.1046/j.1471-

6712.2002.00069.x

Pallone, S. R., & Bergus, G. R. (2009). Fertility awareness-based methods: another option for family planning. *Journal of the American Board of Family Medicine : JABFM*, *22*(2), 147–157. https://doi.org/10.3122/jabfm.2009.02.080038

Smolensky, M. H., & Alonzo, G. E. D. (1993). *Medical Chronobiology : Concepts and Applications*. *147*.

Smoley, B. A., Pendleton, C., Robinson, C. M., Lemoore, N. H., & Station, L. (2012). *Natural Family Planning*.

Su, H.-W., Yi, Y.-C., Wei, T.-Y., Chang, T.-C., & Cheng, C.-M. (2017). Detection of ovulation, a review of currently available methods. *Bioengineering & Translational Medicine*, *2*(3), 238–246. https://doi.org/10.1002/btm2.10058

Sumriddetchkajorn, S., & Chaitavon, K. (2009). Field test studies of our infrared-based human temperature screening system embedded with a parallel measurement approach. *Infrared Physics and Technology*, *52*(4), 119–123. https://doi.org/10.1016/j.infrared.2009.04.002

Watanabe, M., Nakamura, Y., Tomiyama, C., & Abo, T. (2016). *A Specific Pattern in the Basal Body Temperature Chart during the First Week of Pregnancy May Warn of a Miscarriage Crisis*. *May*, 723–729.